Electrochemical Approach to the Repair of Oxetanes Mimicking DNA (6−4) Photoproducts

Fabien Boussicault and Marc Robert*

Laboratoire d'Electrochimie Moléculaire, Université de Paris 7—Denis Diderot, UMR CNRS 7591, Case Courrier 7107, 2 place Jussieu, 75251 Paris Cedex 05, France

Received: April 20, 2006; In Final Form: August 22, 2006

Electrochemical study of oxetanes mimicking DNA (6−4) photoproducts gives new insight into the repair mechanism by (6−4) photolyase. Both electrochemical oxidation and electrochemical reduction at carbon electrodes lead to the cleavage of the oxetanes in a retro-Paterno−Büchi sequence. Within the family of compounds investigated and the range of driving forces offered, transient formation of unstable radical ions is observed, for both oxidative and reductive cleavage. Taking advantage of the electrochemical signature of these mimics, enzymatic assay with *Escherichia coli* CPD photolyase coupled to electrochemical monitoring of the reaction brings evidence that enzymatic repair of (6−4) DNA photoproducts does involve a catalytic dissociative electron-transfer mechanism at the level of an oxetane intermediate.

Introduction

Dissociative electron transfers (DETs) are proved or suspected to be key step events in many natural processes involving redox enzymes. One may cite the study of anaerobic bacteria producing several reductive dehalogenase enzymes that couple the reductive dehalogenation of tetrachloroethylene and other major chlorinated organic pollutants to energy conservation (dehalorespiration).[1] Among these enzymes, *Sulfurospirillum multivorans* catalyzes the reductive dehalogenation of tetrachloroethylene and trichloroethylene to (*Z*)-1,2-dichlorethylene with very high specific activities along a process involving the breaking of two C−Cl bonds.[2] Another example concerning the coupling between electron transfer and bond cleavages is given by DNA photodimer repair by photolyase enzyme, within which the normal base sequence is restored during a sequence involving a photoinduced one-electron reduction associated with the breaking of two C−C bonds in cyclobutane−pyrimidine dimers (CPDs) and of a C−C bond and a C−O bond in a pyrimidine−pyrimidone adduct ((6−4) photoproduct, Figure 1).[3]

This example is important since UV light (200−300 nm) exposition of cells may lead to strong damage of the genome. Although statistically 4 times less frequent than the CPD lesion, (6−4) photoproducts are believed to be severely mutagenic.[3b,4] In addition to the classical excision repair mechanism, redox photolyase enzymes are also able to revert the UV-induced photoproducts to their normal base structure in a catalytic electron-transfer cycle.[3,5,6] (6−4) photolyases are specific enzymes to (6−4) photoproducts, but they share structural homology with the CPD photolyases that revert pyrimidine−cyclobutane dimers. With both enzymes, a dissociative electron transfer to the lesion is supposed to occur inside the catalytic site from the singlet excited state of a fully reduced flavin, $FADH^-$.[3a,5b−d] After cleavage of two covalent bonds and subsequent formation of one neutral base and one reduced base, the catalytic loop closes by electron return from the reduced base to the flavin radical $FADH^{\bullet}$.

This mechanism is only speculative for the repair of (6−4) photoadducts. It has been proposed that charge transfer would not occur directly to the lesion but may rather involve an oxetane intermediate, which would be formed after lesion binding to the enzyme, thanks to the presence of two histidine residues catalyzing a rearrangment in a protonation/deprotonation-driven sequence (Figure 2).[5e] Charge transfer, the key step in the repair, has not been observed until now. Electron transfer has been demonstrated to occur efficiently under UV illumination within a model oxetane covalently linked to a fully reduced deprotonated flavin[7a,b] or tryptophan.[7c] Quantum calculations also suggest that oxetanes quickly cleave after one-electron reduction or oxidation.[8] Photoinduced reactions on model compounds through the use of flash photolysis techniques have shown that

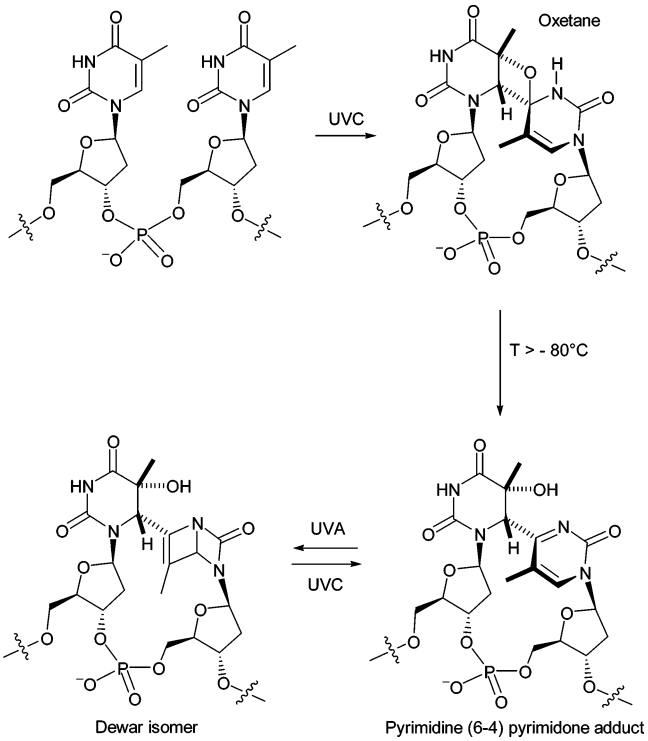

Figure 1. (6−4) photoproduct from UV-induced dimerization of pyrimidine bases in DNA at TT sites.

* To whom correspondence should be addressed. E-mail: robert@paris7.jussieu.fr.

10.1021/jp062425z CCC: $33.50
Published on Web 10/03/2006

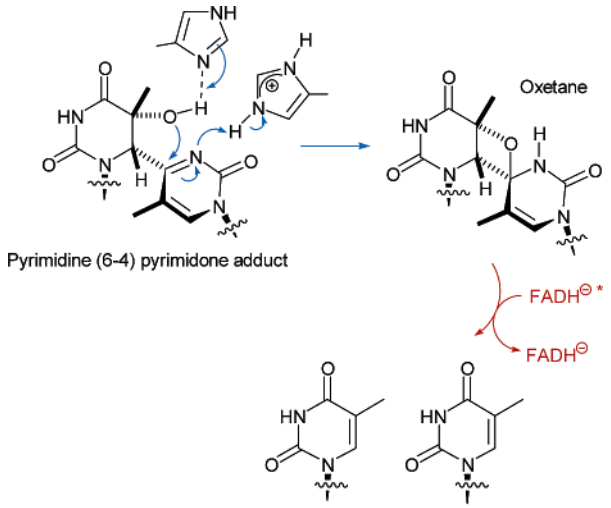

Figure 2. Hypothetic two-step catalytic repair of the (6−4) DNA photoproduct (blue, oxetane formation; red, catalytic dissociative electron-transfer cycle).

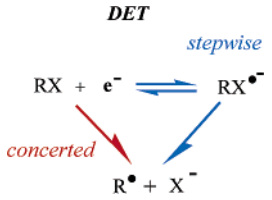

Figure 3. Electron-transfer reaction coupled to bond breaking between heavy atoms (DET). Case of a reduction process. Concerted (red) and sequential (blue) pathways.

CHART 1

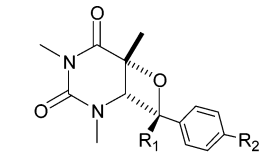

cleavage follows charge-transfer injection from various donors offering a range of driving forces.[9]

To gain new insight into the repair mechanism of (6−4) photoproducts, we studied model compounds using an electrochemical experimental approach, as recently done with pyrimidine dimers mimicking a UV-induced DNA lesion.[10] The oxetanes investigated are shown in Chart 1. The first task of this work was to study their heterogeneous reduction at glassy carbon electrodes in *N*,*N*-dimethylformamide (DMF) and their oxidation in acetonitrile (ACN) and to decipher the exact mechanisms by which these compounds are eventually cleaved. When charge transfer is coupled to a bond-cleavage reaction, the two events may occur concertedly (concerted dissociative electron transfer, CDET) or in two successive steps, the electron transfer then leading to a frangible species that cleaves in a distinct and purely chemical step endowed with an activation barrier (sequential dissociative electron transfer, SDET). [11] Sequential cleavage of ion radicals may occur in a homolytic or heterolytic manner, and in both cases the cleavage amounts to an intramolecular dissociative electron-transfer reaction.[11,12] The two pathways are sketched in Figure 3.

Among our molecules, it appears that both electron injection and removal lead to the cleavage of the oxetane motif, and always along multistep sequential pathways. In the analysis of the experimental data, we took advantage of the synergistic use of quantum calculations to gain physical insight and to better rationalize the cleavage processes. Thanks to the electrochemical signature of the oxetanes, enzymatic assay with *Escherichia coli* CPD photolyase then allowed us to obtain new evidence that (6−4) photoproduct repair likely goes through dissociative charge transfer to an oxetane intermediate.

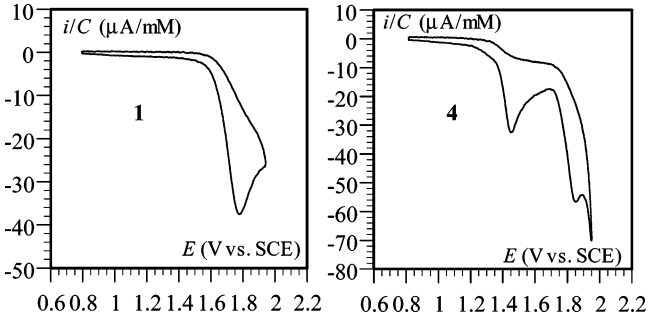

Figure 4. Cyclic voltammetry of oxetanes **1** (left) and **4** (right) on a GC electrode, in ACN + 0.1 M *n*-Bu_4BF_4. Scan rate 0.1 V/s. Temperature 20 °C. On the vertical axis, current normalized versus concentration.

Results and Discussion

Heterogeneous Oxidative Cleavage of Oxetanes Mimicking (6−4) DNA Photoproducts. Typical cyclic voltamograms of compounds **1** and **4** obtained in ACN at a low scan rate on a millimetric glassy carbon (GC) electrode are shown in Figure 4. A single wave is observed with oxetanes **1**−**3**, while two are obtained with **4**. With the latter compound, the second oxidation peak (E_p = 1.85 V vs SCE at 0.1 V/s) closely matches the *N*,*N*-dimethylthymine oxidation signal, in shape, height, and location. This shows that removal of one electron from **4** leads to a retro-Paterno−Büchi process on the first wave, with successive homolytic cleavage of C−C and C−O bonds and formation of a thymine base along with the radical cation of *p*-methoxybenzaldehyde (Figure 5).

The first wave (E_p = 1.44_5 V vs SCE at 0.1 V/s) is thin and smoothly drives to positive potentials as the scan rate is increased ($\partial E_p/(\partial \log \upsilon)$ = 44 mV), indicating an E + C process; i.e., the first electron transfer is followed by a fast and irreversible chemical reaction.[13] This means that charge transfer and bond breaking are successive events (SDET) and not concerted (CDET) and the oxidation goes through an unstable radical cation intermediate that further undergoes rapid cleavage (Figure 5). The electron stoichiometry of the wave is slightly above 1 and was inferred from comparison with the fully reversible wave of a standard redox compound (benzoquinone), for which the following equation applies:[14]

$$i_p^{1e,rev\upsilon} = 0.446 \times FSC^0 D_{\text{standard}}^{1/2} \left(\frac{F\upsilon}{RT}\right)^{1/2} \qquad (1)$$

In the case of the oxetane the overall number of electrons *n* is given by

$$i_p^{ne,irr} = n \times \psi_p FSC^0 D_{\text{substrate}}^{1/2} \left(\frac{F\upsilon}{RT}\right)^{1/2} \qquad (2)$$

i_p = peak current, S = electrode surface area, $C°$ = bulk concentration, D = diffusion coefficient, υ = scan rate, and ψ_p = nondimensional peak current. The nondimensional peak current, ψ_p, was obtained from the peak width, $E_{p/2} - E_p$, at each scan rate.[14]

With oxetanes **1**−**3**, only one bielectronic anodic wave is observed. The oxidation is more difficult than with **4**, as

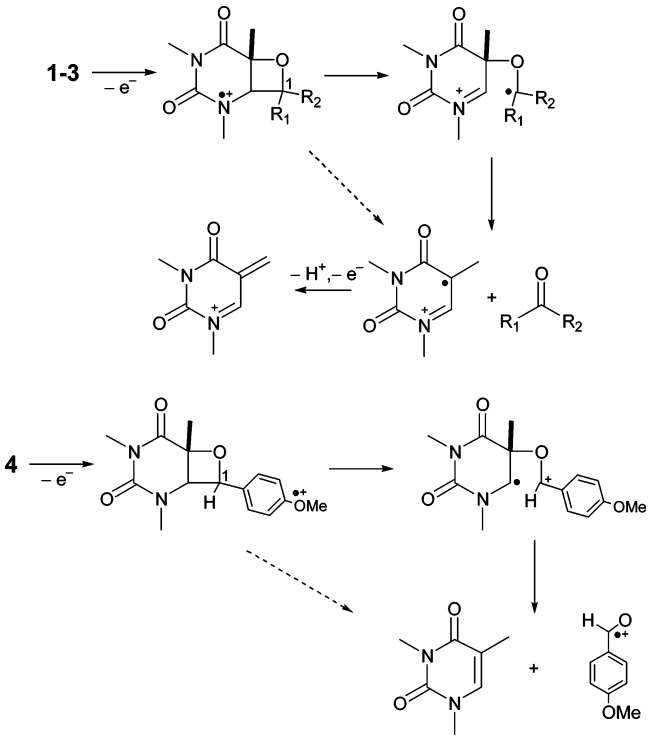

Figure 5. Oxidation mechanism of oxetanes **1**−**4**.

TABLE 1: Votlammetric Data for Oxidation of Oxetanes 1−4

compd	E_p[a]	ΔE[b]	$\partial E_p/(\partial \log v)$[c]	n[d]
1	1.77	75	52	1.95
2	1.70	65	44	2.2
3	1.60_5	55	43	1.85
4	1.44_5	45	44	1.35[e]

[a] In volts vs SCE, at 0.1 V/s. [b] Peak width ($E_{p/2} - E_p$) at 0.1 V/s. [c] In millvolts per decade. [d] Electron stoichiometry. [e] First oxidation wave.

reflected by the more positive values of the peak potential, ranging from 1.60 to 1.77 V vs SCE at low scan rates when going, respectively, from **3** to **2** and finally to **1**. These three oxetanes are oxidized at the nitrogen atom linked to the oxetane motif. The radical cation of the thymine is formed along with an aldehyde (**2**, **3**) or a benzophenone (**1**) after homolytic C−C and C−O bond cleavages, similarly to what was already observed with cyclobutane dimers mimicking DNA base adducts (Figure 5).[10] The radical cation of *N*,*N*-dimethylthymine, produced in the vicinity of the electrode surface, subsequently loses a second electron, since it is more easily oxidized than the thymine itself, thus leading to an overall two-electron process. This second charge transfer is coupled to a proton loss, as shown previously.[10] That the oxidation does not occur at the aromatic substituent borne by the C(1) atom with **1**−**3** at variance with oxetane **4** is attested by the absence of the oxidation wave of neutral *N*,*N*-dimethylthymine, which would be produced in this case. This behavior reflects the fact that the substituents on C(1) are more difficult to oxidize than the *p*-methoxybenzene group present in compound **4**.

The electron stoichiometry for oxetanes **1**−**3** was again inferred from comparison with the reversible wave of benzoquinone. In all three cases, the oxidation peak is thin and drives toward positive potential by a few tens of millivolts per decade log v (see Table 1), which indicates an E + C process with mixed kinetic control between the first electron transfer and the following chemical reaction, leading to the cleavage of the

CHART 2

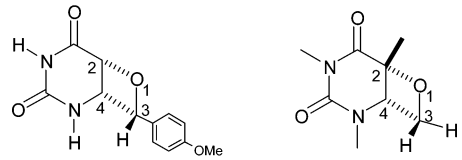

5 **6**

oxetane cation radical. Oxidation thus follows a sequential mechanism (SDET), as with **4**. It was not possible to observe directly the radical cations upon raising the scan rate because of fast cleavage and relatively slow electron transfer. However, since the peak potential location and width are jointly controlled by charge-transfer and bond-cleavage rates, simulation of the voltammetric curves allows estimation of the standard potential $E°$ for the electron release and the rate constant k_c for the cleavage step.[15] Provided the heterogeneous charge-transfer rate constant k_s is known or estimated,[15b] $E°$ and k_c are adjusted to obtain simulated curves that fit experimental variations of both E_p and $E_p - E_{p/2}$ vs log v over the whole range investigated. With **1** and **2**, the standard potentials were estimated to be 1.92 and 1.84 V vs SCE, respectively, while the cleavage rate constant amounts to 10^8 s^{-1} for $\mathbf{1}^{\bullet+}$ and 2.2×10^6 s^{-1} for $\mathbf{2}^{\bullet+}$, close to the value previously obtained for the cleavage of the radical cation of the *cis-anti-N*,*N*-dimethyluracil dimer.[10]

Modeling calculations on compounds $\mathbf{5}^{\bullet+}$ and $\mathbf{6}^{\bullet+}$ (Chart 2) give insight to better rationalize the observed mechanisms. The density functional calculations (B3LYP/6-31G*) were performed to obtain a qualitative picture of the processes and to help answer the following two questions: Which bond cleaves first? Why are cleavages endowed with an activation barrier?

At the equilibrium geometry for $\mathbf{5}^{\bullet+}$, the spin density is essentially (0.74) located on the *p*-methoxyphenyl substituent. A transition state was then identified connecting to the equilibrium geometry on one hand and to a uracil plus the radical cation of *p*-methoxybenzaldehyde on the other hand. At the transition state (TS), the C(3)−C(4) bond length has increased to 2.022 Å (1.667 Å at equilibrium) while the spin density on the phenyl moiety has decreased to approximately 0.39 with a concomitant increase at the C(4) atom (from 0.07 at equilibrium to 0.27 at the TS). The free enthalpy of activation $\Delta G^{\ddagger} = 0.087$ eV, while inclusion of solvent effects through a COSMO calculation leads to a value of 0.19 eV in acetonitrile as a dielectric medium. No other minimum was found on the reaction pathway; in particular no barrier was identified for the second homolytic cleavage of the C−O bond (Figure 6). These observations point to the idea, as already evoked for similar systems,[12a] that the homolytic cleavage of the C(3)−C(4) bond implies an electron transfer from a singly occupied π orbital located on the *p*-methoxyphenyl substituent to the $\sigma_{C(3)-C(4)}$* orbital. Mixing of the two electronic states at the transition state occurs through overlap of the corresponding orbitals that have favorable geometries since the scissile C−C bond lies almost perpendicular to the aromatic plane. This electron transfer is the main reason cleavage goes through a barrier.

In model **6**, no aromatic group is anchored at the C(3) position. Its oxidation should mimic oxidation of oxetanes **1**−**3**. It also closely resembles the oxidation of pyrimidine−cyclobutane dimers. Starting from a minimum on the potential surface ($d_{C(3)-C(4)} = 1.553$ Å), a TS was identified, connecting to a uracil radical cation plus a formaldehyde on the product side. At the TS, the C(3)−C(4) bond length has increased to 2.032 Å and the spin density, initially located on the uracil motif (0.7), has become mainly concentrated on the C(3) atom of the C−C

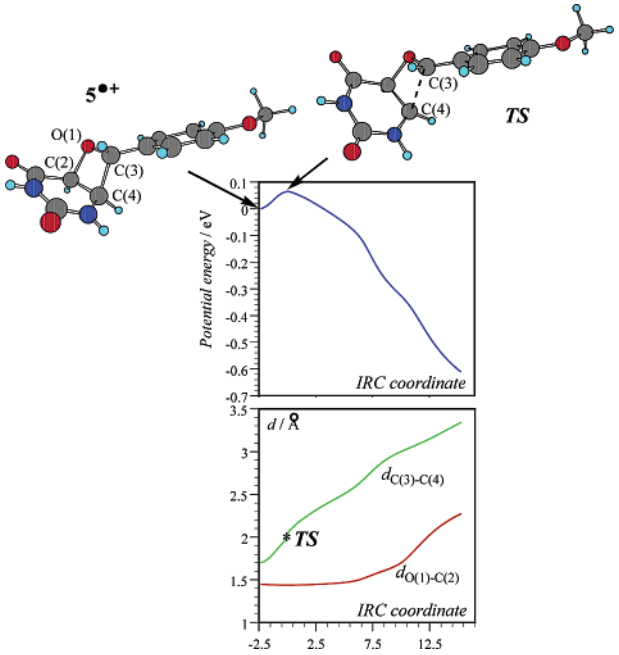

Figure 6. Potential energy surface (gas phase) for oxidative cleavage of **5** (top). Structures at equilibrium (**5**•+) and transition state (TS). Variation of characteristic bond distances during cleavage (bottom). IRC coordinate in $u^{-1/2}a_0$. Atoms: gray, carbon; red, oxygen; blue, nitrogen; light blue, hydrogen.

TABLE 2: Voltammetric Data for Reduction of Oxetanes 1−4

compd	E_p[a]	ΔE[b]	$\partial E_p/(\partial \log v)$	n[c]
1	−2.40	50	−51	2.9
2	−2.41	55	−48	2.5
3	−2.41	55	−52	2.5
4	-2.34_5	90	−74	1.7

[a] In volts vs SCE, at 0.1 V/s. [b] Peak width ($E_{p/2} - E_p$) at 1 V/s. [c] Electron stoichiometry.

cleaving bond (0.56). The free energy of activation amounts to 0.219 eV and marginally increases after solvation is taken into account ($\Delta G^{\ddagger} = 0.237$ eV, COSMO method in acetonitrile). As with **5**•+, no barrier was identified for the subsequent C−O bond cleavage. The reaction leads to an overall retro-Paterno−Büchi sequence with two successive homolytic cleavages, the first one being endowed with an activation barrier due to charge transfer from a π-like orbital to the σ_{C-C}* orbital of the cleaving bond. These calculations are in agreement with the regioselectivity observed during electrochemical oxidation: the first electron is removed from the aromatic *p*-methoxyphenyl substituent with oxetane **4**, while oxidation occurs at the pyrimidine motif with **1**−**3** (Figure 5).

Heterogeneous Reductive Cleavage of Oxetanes Mimicking (6−4) DNA Photoproducts. All four oxetanes are reduced within a single irreversible and very negative wave (ranging from −2.35 to −2.41 V vs SCE at 0.1 V/s; see Table 2). That the reductive process indeed leads to oxetane cleavage is inferred from the observation upon reversal scanning of a small oxidation peak corresponding to the oxidation of the radical anion of the carbonyl compound $R_1R_2C(1)$═O (compounds **2**−**4**).

With **1**, no oxidation was observed on reverse scan because the radical anion of benzophenone is produced at a potential at which it is further reduced. As expected, this oxidation signal disappears in the presence of an added acid, since the radical anion is then readily protonated. To avoid father−son reactions, a few equivalents of a weak acid (2,2,2-trifluoroethanol or acetic acid) was systematically added to the solution. Typical cyclic voltammograms obtained with **1** and **2** in DMF at a low scan rate on a glassy carbon electrode are shown in Figure 7.

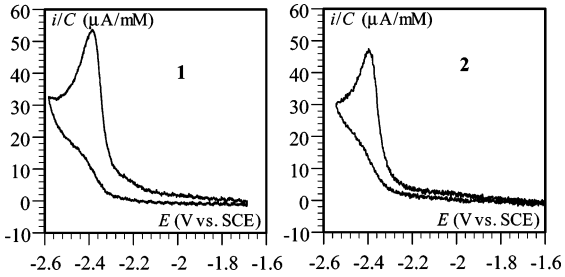

Figure 7. Cyclic voltammetry of oxetane **1** + 4 equiv of 2,2,2-trifluroethanol (left) and of oxetane **2** + 10 equiv of 2,2,2-trifluroethanol (right) on a GC electrode, in DMF + 0.1 M *n*-Bu_4BF_4. Scan rate 0.1 V/s. Temperature 20 °C. On the vertical axis, current normalized versus concentration.

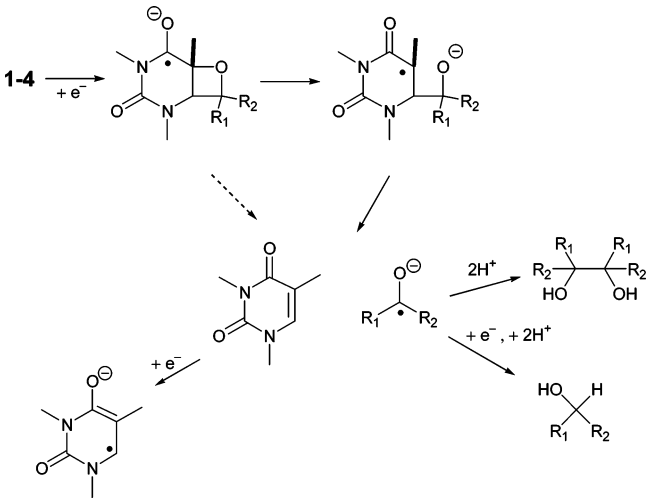

Figure 8. Reduction mechanism of oxetanes **1**−**4**.

From the width of the reduction wave ($E_{p/2} - E_p = 50$ mV at a low scan rate) and peak potential displacement with the scan rate (−51 mV per decade log v), it can be concluded that an E + C mechanism is followed with **1**, the first electron transfer being followed by a fast and irreversible chemical reaction. Reductive cleavage goes through a sequential process (SDET) involving successive electron transfer, heterolytic cleavage of the C−O bond in the radical anion intermediate, and finally homolytic cleavage of a C−C bond, thus leading to the formation of a thymine plus the radical anion of benzophenone. Using the same methodology as for anodic waves, the electron stoichiometry is calculated to equal 3. After bond cleavages, thymine[10] and benzophenone radical anion are reduced with one electron, since they are generated at a potential at which both are reducible.

The reduction mechanism followed with oxetanes **2**−**4** in an acidic medium containing a few equivalents of a weak acid is similar, except for the electron stoichiometry, which lies between 2 and 3, as a result of the fact that the aldehydes obtained in these cases are more basic and less sterically hindered, thus favoring pinacol formation at the expense of the alcohol (Figure 8). All experimental data are gathered in Table 2. It was not possible to obtain the rate constants for fragmentation of radical anion intermediates. At this point, it is worth noting that the mechanistic picture emerging from our data falls in line with previous photoinduced electron-transfer studies.[7c,9] The main difference is that the driving forces offered to the reaction are smaller in our experiments.

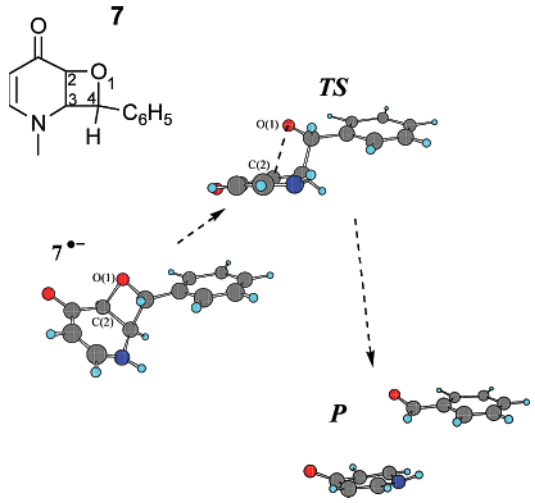

Figure 9. Reductive cleavage of **7**. Structures at equilibrium (**7**•−), transition state (TS), and fragmented products (P). Atoms: gray, carbon; red, oxygen; blue, nitrogen; light blue, hydrogen.

Calculation at the B3LYP level on the very simplified model **7**•− (Figure 9) leads to the following qualitative picture: a minimum corresponding to a stable radical anion was identified with the spin density essentially located on the heterocycle; then a small activation barrier allows a transition state corresponding to the heterolytic cleavage of the C(2)−O(1) bond of the oxetane motif to be reached ($\Delta G^{\ddagger} = 0.12$ eV in the gas phase and was reduced to 0.02 eV after solvation in acetonitrile). Afterward, the energy continuously decreases until formation of the retro-Paterno−Büchi fragments (a neutral heterocycle with two C═C bonds plus the radical anion of benzaldehyde; see Figure 9). En route to the products, homolytic scission of the C(3)−C(4) bond occurs with no activation barrier.

Electrochemical Clues in Understanding the Enzymatic Repair Mechanism. Enzymatic repair of the (6−4) photoproduct has been proposed to proceed via dissociative reduction of an oxetane intermediate with a fully reduced deprotonated flavin acting as a donor. The thermally stable open form of the (6−4) photoproduct would be converted through the less stable oxetane form inside the enzymatic pocket thanks to two histidine residues, as demonstrated for *Xenopus* (6−4) photolyase.[5e] Formation of the four-membered ring intermediate is proposed to follow a sequence illustrated in Figure 2. Mutations of the two identified residues result in an almost complete loss of repair activity.[5e] Support that repair does proceed through dissociative electron transfer came from studies of photoinduced splitting of model oxetanes covalently linked to riboflavin by Carell et al.[7a,b] Nevertheless, such a repair mechanism remains speculative, and direct evidence for its occurrence is lacking.

We have recently discovered that in vitro repair of pyrimidine−cyclobutane dimers by *E. coli* CPD photolyase could be monitored by using electrochemistry.[16] Briefly, argon-deaerated samples (20 μL) in 20 mM Tris−HCl buffer (pH 7.8), 1 mM EDTA, 10 mM dithiothreitol, 50 mM NaCl, and 25% (v/v) glycerol, containing 25 μg of photolyase and *cis-syn*-dimethylthymine dimer (*c-s*-DMT−DMT, 30 mM), were irradiated with a 100 W xenon lamp. Wavelengths below 360 nm were filtered, and repair was followed by monitoring the electrochemical oxidation response of the dimer at a millimetric glassy carbon electrode, after the aliquots had been diluted 100 times in acetonitrile. A typical voltammogram obtained after irradiation (40 min) is reported in Figure 10 (left), showing an approximately 55% repair of the model lesion. The oxidation wave observed around +1.7 V indeed corresponds to dimer cleavage[10] and may

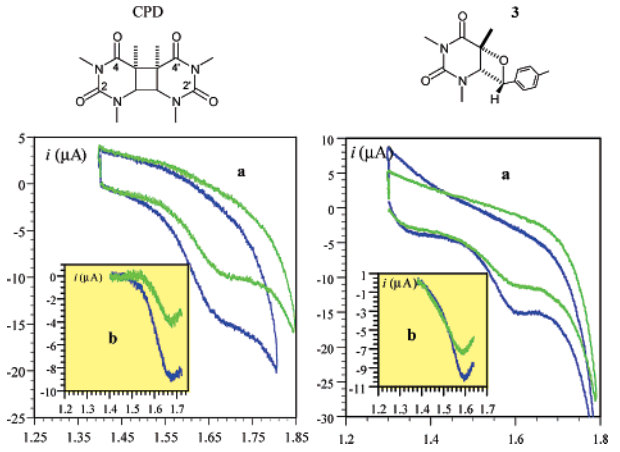

Figure 10. Cyclic voltammetry of the *cis-syn*-dimethylthymine dimer (CPD; left) and oxetane **3** (right) in the presence of *E. coli* CPD photolyase on a GC electrode (blue, before irradiation; green, after irradiation). Substrate concentration before irradiation ~0.3 mM. Scan rate 0.2 V/s. Temperature 20 °C. (a) Raw data. (b) Data after baseline subtraction. On the horizontal axis, potentials referred to SCE.

thus serve as a probe for enzymatic repair. Control experiments confirm that all three ingredients enzyme, substrate, and light are necessary for repair to occur. There is no decrease of the dimer concentration within solutions kept in the dark and containing both the enzyme and the substrate nor for a substrate solution irradiated with light in the absence of enzyme. Equilibrium binding constants of *E. coli* photolyase with dinucleotide dimers are substantially less than with the dimer inserted into the DNA strand, typically 10^3 to 10^4 M^{-1} for the former and 10^7 to 10^8 M^{-1} for the latter.[17] With *c-s*-DMT−DMT, hydrogen bond interactions between the C(2) (C(2′)) and C(4) (C(4′)) carbonyl groups of the two thymine moieties with active residues and water molecules inside the catalytic site maintain some affinity between the enzyme and dimer,[6] and consequently photorepair remains effective.

If (6−4) photolyase enzymes are to repair the (6−4) lesion via electron transfer to an oxetane intermediate, it would likely involve the flavin as an electron donor. However, (6−4) photolyase does not bind thermally stable closed analogues of (6−4) adducts.[5c] If CPD photolyase were able to bind oxetane dimers, even weakly, it would lead to the formation of a complex containing the components involved in the postulated key step for (6−4) adduct repair. We thus prepared a solution containing both *E. coli* CPD photolyase and oxetane **3** in the same experimental conditions as those described above. In the absence of light, the oxetane concentration remains constant, while irradiation at wavelengths above 360 nm leads to an effective repair, as shown from the decrease of the oxidative signal of the oxetane (Figure 10, right). About 30% of the substrate is repaired after 60 min of irradiation, slightly below the repair efficiency measured with *c-s*-DMT−DMT. It was also checked that irradiation of **3** in the absence of enzyme does not lead to cleavage and formation of thymine. These striking observations could be ascribed to a dissociative electron-transfer process involving as a donor the excited state of a fully reduced flavin. Hydrogen bonds with active site residues and its size allow the oxetane to fit in the catalytic site. We believe these results provide evidence that (6−4) pyrimidine−pyrimidone DNA photoproducts are repaired by (6−4) photolyase through an electron transfer coupled to C−O and C−C bond cleavages of an oxetane intermediate.

One issue remaining concerns the concerted or sequential nature of the dissociative electron-transfer sequence during repair

in both CPD and (6−4) photolyases. Despite recent direct observation of cyclobutane−pyrimidine dimer repair dynamics in the picosecond time domain,[3f] both pathways may account for the high quantum yield of repair ($\phi \approx 0.9$).[3a] It seems even more difficult to conclude for (6−4) photoproduct repair. From the low quantum yield measured with *Xenopus* (6−4) photolyase ($\phi \approx 0.11$),[5d] it may be inferred that repair is controlled, at least in part, by the oxetane formation step. If this were not the case, the quantum yield would mainly depend on the sequential or concerted nature of the dissociative electron-transfer catalytic cycle. In the case of a sequential mechanism involving transient formation of a radical/radical anion pair ($FADH^{\bullet}$/oxetane$^{\bullet-}$), the reducing power of the excited state of the flavin $FADH^{-}$* ($E°(FADH^{\bullet}/FADH^{-}*) \approx -2.92$ V vs SCE)[18] on one hand and that of the radical anion of the oxetane ($E° \geq -2.5$ V vs SCE)[19a] on the other indicate not only that the formation of the $FADH^{\bullet}$/oxetane$^{\bullet-}$ pair would be very efficient but also that back electron transfer, lying deep in the Marcus inverted region ($\Delta G^{\circ,\mathrm{back}} = E°(\text{oxetane/oxetane}^{\bullet-}) - E°(FADH^{\bullet}/FADH^{-}) \ll -\lambda$),[19b] would certainly not compete with bond cleavage. Quantum yields on the order of those measured during CPD repair should then be obtained. In the hypothesis of a fully concerted pathway, the quantum yield would be higher than 0.5.[20] Thus, during the repair process, oxetane formation inside the catalytic site may be not very efficient and/or the remaining open form of the (6−4) photoproduct may be partly converted into its Dewar valence isomer during irradiation, lowering the repair efficiency.

Conclusion

Electrochemical reduction and oxidation of oxetanes **1**−**4** lead to their cleavage. Oxidation in ACN occurs at very positive potentials and involves the formation of a transient radical cation that cleaves in a second step consisting of an intramolecular dissociative electron transfer. With compounds **1**−**3**, oxidation takes place at the pyrimidine site, thus leading, after breaking of the oxetane motif, to the formation of the radical cation of *N*,*N*-dimethylthymine and of a neutral carbonyl molecule (benzophenone or aldehyde). With **4**, the first electron is removed from the *p*-methoxybenzene substituent, and thus, the fragments obtained are a neutral thymine and the radical cation of *p*-methoxybenzene. In all four cases, the reaction involves the homolytic breaking of a C−C bond of the oxetane motif that is not concerted with charge transfer and then the cleavage of the C−O bond. From the shape of the voltammograms, the rate constant for cleavage of the cation radicals ($\mathbf{1}^{\bullet+}$, $\mathbf{2}^{\bullet+}$) was estimated to be in the submicrosecond range. Reduction of the oxetanes in DMF also leads to a retro-Paterno−Büchi process along which the C−O and C−C bonds of the oxetane motif are successively cleaved. The extra electron first locates on the thymine part of the substrate, and then the radical anion intermediate dissociates in a heterolytic manner. The neutral thymine formed then takes a second electron since it is produced at a potential where it is reducible. The cleavage rate constants could not be obtained. Enzymatic assay with *E. coli* CPD photolyase coupled to an electrochemical detection of oxetane **3** then allowed observation of an effective repair of the model lesion, bringing evidence that enzymatic repair in (6−4) photolyase goes through a dissociative electron transfer to an oxetane intermediate.

Experimental Section

Chemicals. *N*,*N*-Dimethylformamide (Fluka, >99.5%, stored on molecular sieves and under an argon atmosphere), acetonitrile (Fluka, >99.5%, stored on molecular sieves and under an argon atmosphere), the supporting electrolyte NBu_4BF_4 (Fluka, puriss), thymine (Sigma, 99%), benzophenone (Prolabo), benzaldehyde (Aldrich, 99+%), tolualdehyde (Aldrich, 97%), anisaldehyde (Aldrich, 98%), acetic acid (Prolabo, Normapur), 2,2,2,-trifluoroethanol (Aldrich, 99.5+%), cyclohexane (Prolabo, Normapur), ethyl acetate (Prolabo, Normapur), and silica gel (Macherey Negel) were used as received.

E. coli CPD photolyase enzyme was purchased from Trevigen. The enzyme was fractioned in working aliquots of 10 μL each and stored at −80 °C. Before the experiment, the aliquots were allowed to slowly defrost in ice for 1 h and diluted in a working buffer containing the substrate.

Synthesis. Oxetanes **1**−**4** were synthesized as previously described.[9b] Briefly, *N*,*N*-dimethylthymine (2 mmol) and aromatic carbonyl compound (4 mmol) were dissolved in 20 mL of acetonitrile and placed in a quartz tube. After O_2 was purged with argon for 30 min, the mixture was irradiated using the unfiltered output of a 150 W Xe lamp for 5 h. The compounds were purified over silica gel using ethyl acetate/cyclohexane (20/80 to 40/60, v/v) as eluent and finally characterized as pure products by ^{1}H NMR.[9b]

Instrumentation. The working electrode was a 3 mm diameter glassy carbon electrode disk (Tokai) carefully polished and ultrasonically rinsed in absolute ethanol before use. The counter electrode was a platinum wire and the reference electrode an aqueous SCE electrode. The potentiostat, equipped with positive feedback compensation and a current measurer, used at low or moderate scan rates, was the same as previously described.[21] All experiments were done at 20 °C, the double-wall jacketed cell being thermostated by circulation of water.

Quantum Chemical Calculations

All the calculations were performed with the Gaussian 98 series of programs.[22] The DFT (B3LYP) method and 6-31G* basis set were used. Minimum-energy structures were fully optimized. Frequency calculations were made to verify that the structures were minima (no imaginary frequencies) or saddle points (one imaginary frequency) and to evaluate thermodynamical functions. The nature of the reactant and products linked to transition states was assigned by the intrinsic reaction coordinate (IRC) method at the same level of calculation as used for saddle point characterization. IRCs have been determined in mass-weighted internal coordinates with a step size of 0.05 or 0.1 in atomic units. The activation barriers were calculated as the free enthalpy difference between the saddle point and the minimum structures.

Acknowledgment. This work was supported by the French Ministère de la Recherche et des Nouvelles Technologies (Young Investigator Program "ACI Jeune Chercheur") and CNRS (Centre National de la Recherche Scientifique).

References and Notes

(1) (a) Neumann, A.; Scholz-Muramatsu, H.; Diekert, G. *Arch. Microbiol.* **1994**, *162*, 295. (b) Wohlfarth, G.; Diekert, G. *Curr. Opin. Biotechnol.* **1997**, *8*, 290.

(2) Diekert, G.; Gugova, D.; Limoges, B.; Robert, M.; Savéant J.-M. *J. Am. Chem. Soc.* **2005**, *127*, 13583.

(3) (a) Sancar, A. *Chem. Rev.* **2003**, *103*, 2203 and references therein. (b) Taylor, J.-S. *Acc. Chem. Res.* **1994**, *27*, 76. (c) Heelis, P. F.; Hartman, R. F.; Rose, S. D. *Chem. Soc. Rev.* **1995**, 289. (d) Carell, T.; Burgdorf, L. T.; Kundu, L. M.; Cichon, M. K. *Curr. Opin. Chem. Biol.* **2001** *5*, 491. (e) Harrison, C. B.; O'Neil, L. L.; Wiest, O. *J. Phys. Chem A* **2005**, *109*, 7001. (f) Kao, Y.-T.; Saxena, C.; Wang, L.; Sancar, A.; Zhong, D. *Proc. Natl. Acad. Sci. U.S.A.* **2005**, *102*, 16128.

(4) Gibbs, P. E. M.; Kilbey, B. J.; Banerjee, S. K.; Lawrence, C. W. *J. Bacteriol.* **1993**, *175*, 2607.

(5) (a) Todo, T.; Ryo, H. *Mutat. Res.* **1992**, *273*, 85. (b) Kim, S.-T.; Malhotra, K.; Smith, C. A.; Taylor, J.-S.; Sancar, A. *J. Biol. Chem.* **1994**, *269*, 8535. (c) Zhao, X.; Liu, J.; Hsu, D.; Zhao, S.; Taylor, J.-S.; Sancar, A. *J. Biol. Chem.* **1997**, *272*, 32580. (d) Hitomi, K.; Kim, S.-T.; Iwai, S.; Harima, N.; Otoshi, E.; Ikenaga, M.; Todo, T. *J. Biol. Chem.* **1997**, *272*, 32591. (e) Hitomi, K.; Nakamura, H.; Kim, S.-T.; Mizukoshi, T.; Ishikawa, T.; Iwai, S.; Todo, T. *J. Biol. Chem.* **2001**, *276*, 10103.

(6) Mees, A.; Klar, T.; Gnau, P.; Hennecke, U.; Eker, A. P.; Carell, T.; Essen, L.-O. *Science* **2004**, *306*, 1789.

(7) (a) Cichon, M. K.; Arnold, S.; Carell, T. *Angew. Chem., Int. Ed.* **2002**, *41*, 767. (b) Friedel, M. G.; Cichon, M. K.; Carell, T. *Org. Biomol. Chem.* **2005**, *3*, 1937. (c) Song, Q.-H.; Wang, H.-B.; Tang, W.-J.; Guo, Q.-X.; Yu, S.-Q. *Org. Biomol. Chem.* **2006**, *4*, 291.

(8) (a) Wang, Y.; Gaspar, P. P.; Taylor, J.-S. *J. Am. Chem. Soc.* **2000**, *122*, 5510. (b) Izquierdo, M. A.; Domingo, L. R.; Miranda, M. A. *J. Phys. Chem. A* **2005**, *109*, 2602.

(9) (a) Prakash, G.; Falvey, D. E. *J. Am. Chem. Soc.* **1995**, *117*, 11375. (b) Joseph, A.; Prakash, G.; Falvey, D. E. *J. Am. Chem. Soc.* **2000**, *122*, 11219. (c) Joseph, A.; Falvey, D. E. *J. Am. Chem. Soc.* **2001**, *123*, 3145.

(10) Boussicault, F.; Krüger, O.; Robert, M.; Wille, U. *Org. Biomol. Chem.* **2004**, *2*, 2742.

(11) Costentin, C.; Robert, M.; Savéant, J.-M. *Chem. Phys.* **2006**, *324*, 40 and references therein.

(12) (a) Costentin, C.; Robert, M.; Savéant, J.-M. *J. Am. Chem. Soc.* **2003**, *125*, 105. (b) Costentin, C.; Robert, M.; Savéant, J.-M. *J. Am. Chem. Soc.* **2004**, *126*, 16051.

(13) A concerted reaction would have led to much larger waves and variations of the peak potential with log υ substantially larger than 60 mV per decade. The reason is that the kinetics is much slower in a concerted reaction since the intrinsic barrier includes one-fourth of the bond dissociation energy in addition to the solvent contribution.[11]

(14) (a) Nadjo, L.; Savéant, J.-M. *J. Electroanal. Chem.* **1973**, *48*, 113. (b) The diffusion coefficients D were estimated through application of the Stokes−Einstein equation $D = k_BT/(6\pi\eta a)$, η being the solvent viscosity and a the hard-sphere radius equivalent to the radius of the diffusing molecule. Radii were obtained from a quantum calculation at the B3LYP level (keyword "Volume"). This leads to $(D_{standard}/D_{substrate})^{1/2}$ factors ranging from 1.13 to 1.18 in the application of eqs 1 and 2.

(15) (a) See ref 15c for a full description of the fitting procedure. (b) k_s may be estimated to be 0.2 cm/s by comparison with molecules of similar size and charge. (c) Pause, L.; Robert, M.; Savéant, J.-M. *J. Am. Chem. Soc.* **2001**, *123*, 4886.

(16) Boussicault, F.; Clivio, P.; Robert, M. Submitted for publication.

(17) Kim, S.-T.; Sancar, A. *Biochemistry* **1991**, *30*, 8623.

(18) (a) $E^\circ(\text{FADH}\bullet/\text{FADH}^{-*}) \approx -E^*(\text{FADH}^-) + E^\circ(\text{FADH}\bullet/\text{FADH}^-) = -2.76^{3a} - 0.16^{18b} = -2.92$ V vs SCE. (b) Gindt, Y. M.; Schelvis, J. P. M.; Thoren, K. L.; Huang, T. H. *J. Am. Chem. Soc.* **2005**, *127*, 10472.

(19) (a) Although not obtained from voltammetric study, the standard potentials for oxetanes **1**−**4** are likely slightly more negative than the reductive potentials measured at a low scan rate, −2.5 V vs SCE being an approximate but reasonable mean value. Moving to the real oxetane lesion and enzymatic environment should not move this value toward positive potentials by more than a few hundred millivolts. (b) The driving force for back electron transfer is thus predicted to be more negative than −2 eV, while the reorganization energy λ certainly does not exceed 1−1.5 eV.

(20) Robert, M.; Savéant, J.-M. *J. Am. Chem. Soc.* **2000**, *122*, 514.

(21) Garreau, D.; Savéant, J.-M. *J. Electroanal. Chem.* **1972**, *35*, 309.

(22) Frisch, M. J.; Trucks, G. W.; Schlegel, H. B.; Scuseria, M. A.; Gill, P. M. W.; Johnson, B. G.; Robb, M. A.; Cheeseman, J. R.; Keith, T.; Petersson, G. A.; Montgomery, J. A.; Stratmann, R. E.; Burant, J. C.; Dapprich, S.; Millam, J. M.; Daniels, A. D.; Kudin, K. N.; Strain, M. C.; Farkas, O.; Tomasi, J.; Barone, V.; Cossi, M.; Cammi, R.; Mennuci, B.; Pomelli, C.; Adamo, C.; Clifford, S.; Ochterski, G.; Cui, Q.; Morokuma, K.; Malick, D. K.; Rabuck, A. D.; J. A.; Raghavachari, K.; Al-Laham, M. A.; Zakrzewski, V. G.; Ortiz, J. V.; Foresman, J. B.; Cioslowski, J.; Stefanov, B. B.; Liu, G.; Liashenko, A.; Piskorz, P.; Komaromi, I.; Nanayakkara, A.; Challacombe, M.; Peng, C. Y.; Ayala, P. Y; Chen, W.; Wong, M. W.; Andres, J. L.; Replogle, A. S.; Gomperts, R.; Martin, R. L.; Fox, D. J.; Binkley, J. S.; Defrees, D. J.; Baker, J.; Stewart, J. P.; Head-Gordon, M.; Gonzalez, C.; Pople, J. A. *Gaussian 98*, Revision A.1; Gaussian, Inc.: Pittsburgh, PA, 1998.